



LAWRENCE
LIVERMORE
NATIONAL
LABORATORY

Materials and Fabrication Issues for Large Machined Germanium Immersion Gratings

P. J. Kuzmenko, P. J. Davis, S. L. Little, L. C.
Hale

May 23, 2006

Opto-Mechanical Technologies for Astronomy
Orlando, FL, United States
May 24, 2006 through May 31, 2006

Disclaimer

This document was prepared as an account of work sponsored by an agency of the United States Government. Neither the United States Government nor the University of California nor any of their employees, makes any warranty, express or implied, or assumes any legal liability or responsibility for the accuracy, completeness, or usefulness of any information, apparatus, product, or process disclosed, or represents that its use would not infringe privately owned rights. Reference herein to any specific commercial product, process, or service by trade name, trademark, manufacturer, or otherwise, does not necessarily constitute or imply its endorsement, recommendation, or favoring by the United States Government or the University of California. The views and opinions of authors expressed herein do not necessarily state or reflect those of the United States Government or the University of California, and shall not be used for advertising or product endorsement purposes.

Materials and Fabrication Issues for Large Machined Germanium Immersion Gratings

Paul J. Kuzmenko*, Pete J. Davis, Steve L. Little, and Layton C. Hale
Lawrence Livermore National Laboratory, L-183 PO Box 808, Livermore, CA 94551

ABSTRACT

LLNL has successfully fabricated small (1.5 cm² area) germanium immersion gratings. We studied the feasibility of producing a large germanium immersion grating by means of single point diamond flycutting. Our baseline design is a 63.4° blaze echelle with a 6 cm beam diameter. Birefringence and refractive index inhomogeneity due to stresses produced by the crystal growth process are of concern. Careful selection of the grating blank and possibly additional annealing to relieve stress will be required. The Large Optics Diamond Turning Machine (LODTM) at LLNL is a good choice for the fabrication. It can handle parts up to 1.5 meter in diameter and 0.5 meter in length and is capable of a surface figure accuracy of better than 28 nm rms. We will describe the machine modifications and the machining process for a large grating. A next generation machine, the Precision Optical Grinder and Lathe (POGAL), currently under development has tighter specifications and could produce large gratings with higher precision.

Keywords: immersion grating, germanium, diamond machining, stress birefringence

1. INTRODUCTION

The concept of immersing a diffraction grating in a high index transmissive material and the benefits of such a configuration originated over 50 years ago¹. But it has only been relatively recently that instrument builders have begun to realize that immersion gratings bring performance advantages to state of the art optical designs, and can actually be fabricated with high optical quality. Several instruments have been proposed incorporating immersion gratings or grisms into their designs. Because an immersion grating has both dispersion and resolution increased relative to a conventional reflection grating by a factor of the refractive index N , the benefits are most pronounced in the infrared. An immersion spectrometer can offer reduced size while maintaining resolution or increased resolution while maintaining size. The latter will be the focus of this paper.

LLNL has recently achieved high efficiency and excellent optical quality in diamond machining small (1.5 cm²) germanium immersion gratings for the 8 to 13 μm wavelength range². If the size can be scaled up substantially, there could certainly be applications to ground based astronomical instrumentation, in particular, high resolution spectroscopy. This provided the impetus for studying the feasibility of fabricating large immersion gratings by diamond machining.

There has been some prior work in this area. Ebizuka and his colleagues in Japan are working to construct a large germanium echelle (120 x 120 mm entrance aperture, 68.75° blaze, 600 μm groove spacing) for use in a very high resolution mid-infrared spectrometer for the SUBARU telescope³. They use a nanoprecision grinding technique that employs an iron bonded diamond grinding wheel. An electrolytic process along with mechanical truing is used to maintain the sharpness of the wheel and a tight corner radius. Thus far they have fabricated a 1/4 scale grating with acceptable quality for 10 μm operation. This same precision grinding technique is also being studied for application to zinc selenide. Kobayashi and coworkers are proposing a near infrared instrument that would employ a ZnSe grating with a 70° blaze, 35 μm period and a 70 mm entrance aperture⁴.

Another approach to fabricating large immersion gratings is by anisotropic chemical etching. This technique relies on very slow etch rates along certain crystal planes and fast rates along others. In silicon etch rates normal to the (111) crystal plane are nearly 100 times slower than in any other direction. As a result chemical etching creates relatively smooth groove facets parallel to the (111) crystal planes. Ge and his research group at Florida have reported plans to

*Author information: Email: kuzmenko1@llnl.gov; Telephone: (925) 423-4346; Fax: (925) 422-2499

fabricate gratings on 6 inch and ultimately 8 inch diameter substrates of thick silicon⁵. However the anisotropic etching techniques that work very well in single crystal silicon are not applicable other materials. So this process is not as versatile as mechanical fabrication.

As mentioned above, the goal of this paper is to investigate the feasibility of fabricating large immersion gratings in germanium by means of single point, single crystal diamond machining. Our approach is to carry out a design study to identify the critical issues and the limitations of the technology. The first step to determine the parameters of a prototypical grating. This is done in section 2. Next we look at materials limitations both fundamental and practical. This is done in section 3. Section 4 examines current machining capabilities and presents a fabrication plan based on current technologies. Section 5 looks at what may be possible with future machine technology. Conclusions are presented in section 6.

2. SPECIFICATION OF PROTOTYPE GRATING FOR DESIGN STUDY

The use of an immersion grating is most beneficial in high resolution spectroscopy. Working in germanium with a refractive index of about 4, the diffraction-limited resolution is increased by a factor of 4 over an equivalent reflection grating. This is also true for the seeing limited case due to the 4x increased dispersion. Let's baseline a spectrometer with resolution $R \sim 40,000$. For comparison with existing instruments NIRSPEC has a resolution of 25,000 and the Phoenix instrument has demonstrated an R of 75,000. In the diffraction limit an immersion grating spectrometer has a spectral resolution $R = 2nL/\lambda$ where n is the refractive index, L is the length of the grating parallel to the incident beam and λ is the operating wavelength. One can achieve a resolution of 40,000 with a germanium grating of 1 cm length at 2 μm and 5 cm length at 10 μm . However, barring operation outside the atmosphere or the use of a good adaptive optics system, the entrance slit is generally wider than required for diffraction limited operation because the image formed on the slit by the input telescope is not diffraction limited. In this seeing limited case the spectral resolution is given by $R = 2nL/s$ where s is the slit width. If we specify a resolution of 40,000 with a 25 μm wide slit then a germanium grating of 12.5 cm length is needed.

Table 1. Groove spacing for 63.4° blaze angle germanium ($n= 3.93$) echelle as a function of wavelength and pixel format to achieve a spectral resolution of 40,000

	λ (μm)	λ (μm)	λ (μm)	resolution	blaze angle
array width	2.5	5	10	40000	63.4
(pixels)	d(μm)	d(μm)	d(μm)		
2048	13.67	27.34	54.69		
1024	27.34	54.69	109.38		
512	54.69	109.38	218.75		
256	109.38	218.75	437.50		

High resolution spectrometers generally use echelle gratings at high blaze angle to attain high dispersion. A common blaze angle is 63.4° which means that the height of the entrance face is 1/2 the length of the grating. Choosing this blaze for our prototype gives an entrance aperture of just over 6 cm. Good optical practice suggests that the clear aperture of an optical surface be 80% of the total aperture because it is difficult to get good quality out near the edges. Applying this rule gives the external dimensions of the grating as 7.5 x 7.5 x 15 cm in the shape of a right angle prism. The ruled area would be on the hypotenuse with the grooves covering a region 6 cm wide by 13.4 cm long.

It remains to select the groove spacing. A high dispersion echelle is typically paired with an order sorter, a lower dispersion grating or prism set up to cross disperse the echelle orders across a detector array. In this case each order would be aligned with a set of rows of the array. Therefore one requires the number of resolvable wavelengths in an order to correspond to the number of pixels in a row. An example will clarify this. At 5 μm and $R=40,000$ the resolvable spectral width is 0.05 cm^{-1} . If we have 2000 pixels in a row (2048 x 2048 array) and sampling theory requires 2 pixels per resolvable spectral width then the row will cover 50 cm^{-1} . So the spacing between echelle orders should be 50 cm^{-1} . For an immersed echelle with groove spacing d and blaze angle θ , the order spacing is $1/2nd(\sin \theta)$. Taking $n=4$ and a 63.4° blaze, the groove spacing works out to be 28 μm . If a resolution of 40,000 at 10 μm is required the spacing would double to 56 μm . Smaller format focal planes will also require larger groove spacing. See Table 1 for details.

In summary, we have chosen the specifications for a prototypical germanium echelle for an R~40,000 infrared spectrometer. It takes the form of a right angle prism with dimensions of 7.5 x 7.5 x 15 cm. The blaze angle is 63.4°. It will accept a 6 cm diameter beam. Assuming a 2048 x 2048 pixel array and operation around 5 μm yields a groove spacing of about 30 μm .

3. MATERIALS LIMITATIONS

Having set tentative grating specifications, the first issue is the availability of germanium blanks that will meet the optical requirements. One must consider size, crystal orientation, doping, and polycrystalline vs. single crystal, as well as the optical absorption and the optical homogeneity. It is fortunate that germanium has been long used as an infrared optical material for both scientific and defense applications. Although the largest sizes are available in polycrystalline form, we prefer to use single crystal germanium for diamond machining gratings for several reasons. Although germanium is a cubic crystal, properties relevant to the machining process vary along crystal planes. As a result there are crystal orientations that cut faster and yield better surface quality. With a single crystal substrate one can orient the blank for optimal cutting. In polycrystalline material the individual grains can get pulled out during the machining process leaving surface pits. Finally there can be excess scatter at the grain boundaries especially at the shorter wavelengths. Umicore Corporation can supply single crystal germanium in the (111) orientation in a 10 inch diameter boule. Ebizuka reports that TDY, Corp. in Japan fabricated a single crystal 400 mm in diameter and 120 mm thick. Either of these would be large enough for the prototype grating.

An immersion grating is an unusual optical element in that the path length within solid material is quite large, up to 30 cm in the prototype echelle. For good performance, one requires low optical absorption. There are three mechanisms of infrared absorption for germanium: excitation of electrons across the bandgap, multiphonon absorption by the crystal lattice, and absorption by free electrons and holes.

On the short wavelength side there is a fundamental absorption edge due to an indirect band gap (i.e. a phonon must assist in the optical absorption in order to conserve momentum). Due to the thermal distribution in phonon energies the cutoff is not abrupt. At 300K the energy gap corresponds to a wavelength of 1.88 μm but at 2.066 μm there is still an absorption coefficient of 0.04/cm⁶. With cooling the bandgap increases so that at 77K the cutoff has shifted to 1.7 μm . So the short wavelength limit for a large germanium grating would be about 2.1 μm at ambient temperatures and about 1.9 μm for cryogenic operation.

At long wavelengths, 3 phonon lattice absorption begins at about 11.5 μm . Between 11.5 and 14 μm lattice absorption ranges from 0.15 to 0.25/cm at 293 K and from 0.06 to 0.09/cm at 77K and below⁷. This would result in unacceptable absorption in a large grating, imposing a long wave limit of about 11.5 μm .

Absorption from thermally excited, free electrons and holes is the dominant mechanism over the useful wavelength range. It scales as carrier density and the square of the wavelength. Most absorption measurements in germanium have been at the CO₂ laser wavelength of 10.6 μm . Due to a difference in selection rules for holes and electrons, n-type material has the lowest absorption at room temperature. This is the form (optical grade) that is most readily available. Deutsch reported best values 0.012/cm at 10.6 μm and 0.0018/cm at 5.25 μm ⁸. This indicates that optical grade germanium would have acceptable absorption in a large echelle. Near the long wavelength limit, where cryogenic operation would be required, lower absorption should be possible using undoped germanium of the highest purity. In the absence of donor and acceptor impurities, both hole and electron densities drop sharply with temperature.

It is known, but perhaps not too well known, that semiconductor crystals can suffer from inhomogeneities in refractive index. Given the very stringent requirements imposed by the electronics industry, it may seem surprising that such crystals are not nearly "perfect." Indeed the crystals are free of dislocations and other gross defects and impurity levels are extremely low. However, stresses generated during the crystal growth process and locked in after solidification produce changes in refractivity through the stress-optic effect. Strain in a semiconductor crystal shifts the electron distribution to preferentially lie in conduction band valleys aligned with the direction of maximum strain⁹.

In the common Czochralski (CZ) crystal growth technique a small seed crystal is dipped into a crucible of molten material. The crystal is raised very slowly as material solidifies on the outer surface. Germanium expands on

solidification. There is a natural temperature gradient between the center and the outer surface and an axial gradient may be present as well. As the crystal equilibrates to ambient temperatures a radial compressive stress is built up as the outside cools more than the inside. A tensile stress builds up in the tangential direction. See figure 1. Variations in stress with radial position results in refractive index inhomogeneities. Because the stress varies with orientation, significant birefringence is also present.

One reason this phenomenon is not well known is that few measurements have been reported. Interferometric measurements at 10.6 μm on a 100 mm diameter 30 mm thick disc of CZ germanium were reported by Gaskin and Lewis¹⁰. They found a maximum Δn across the sample of 3.1×10^{-4} , which was reduced to 6.7×10^{-5} after annealing. Gafni et al. obtained similar results on 150 to 200 mm diameter samples that were 25 mm thick¹¹. Depuydt and colleagues applied both polarimetry and interferometry at 10.6 μm to large CZ discs 235 mm diameter and 45 mm thick¹². In the region of maximum stress near the edge of the disc a birefringent path difference of $\lambda/2$ was observed between light polarized along the two orthogonal stress components (radial and tangential). Interferometric measurements with the laser polarization aligned along one of the stress components showed a roughly parabolic profile with $\Delta n \sim 0$ at the center. It increased near the edge to 4×10^{-5} for polarization parallel to the tangential stress component and -1.2×10^{-4} for polarization parallel to the radial stress component. Ebizuka et al. measured the homogeneity of a 32 x 32 x 80 mm germanium block for use as a grating blank³. No wavefront error was observed with an interferometer and an InSb camera but the sensitivity limit was not reported.

Some vendors quote typical values for refractive index variation within a component (e.g. Umicore datasheet GeIR/9902 specifies 0.1 to 1.0×10^{-4} for single crystal material), but due to the high cost (~\$200,000) of the infrared interferometer none have the capability to make these measurements in house. If required this data is obtained at other facilities at customer expense. This was done a number of years ago at Umicore¹³. A 1/2 inch thick, double annealed slab of germanium, 3 inches by 30 inches, registered maximum Δn in the range of 6 to 8×10^{-5} .

Are the properties of available germanium adequate for good grating performance? Let's consider the issue of birefringence first. For a grating to function properly, light diffracted by a groove should be able to constructively and destructively interfere with light diffracted from the other grooves. This can only happen if they are in the same or relatively similar polarization states. If their polarization states are orthogonal they will not interfere at all. Because the rays diffracted by different grooves travel different distances in a birefringent material their polarization states will generally differ when they are brought together and they no will longer interfere with 100% extinction. The only exception would be if a linearly polarized beam happened to be aligned with one of the axes of birefringence.

We do not know the initial states of polarization nor their orientation relative to the birefringent axes. Let us assume random polarization by which we mean instantaneously linear polarization whose orientation is rapidly varying but yet slowly with respect to the transit time through the germanium. The birefringent phase shift is given by $\phi = (n_1 - n_2)d/\lambda$, where n_1 and n_2 are the orthogonal refractive indices and d is the path length. So the extinction factor averaged over all orientations of linear polarization is $3/4 + (1/4)\cos \phi$. Therefore 1/4 wave of birefringence gives 75% extinction and 1/2 wave gives the worst case of 50% extinction.

Let's assume that we can tolerate a maximum of $\lambda/4$ of birefringence. Over a 30 cm path the maximum $\Delta n = (n_1 - n_2)$ will be 8.3×10^{-6} at 10 μm and 1.7×10^{-6} at 2 μm . These are very tight constraints. The real situation is not quite this stringent. Recall that achieving a diffraction-limited resolution of 40,000 required a grating length of 5 cm at 10 μm and 1 cm at 2 μm . This is the path length difference over which the diffracted beams should completely interfere and hence the path length over which the birefringence specification must apply. Thus the true constraint on Δn is $\leq 5 \times 10^{-5}$. A grating physically longer than the diffraction limited length provides more throughput but no greater resolution since the resolution is limited by the slit width.

The next issue to examine is that of refractive inhomogeneity. For a grating to work we need to maintain a constant phase relation between light diffracted from each groove. In other words the optical path difference between any pair of adjacent grooves along a given ray direction should be equal. This physical statement is expressed mathematically by the grating equation, $m\lambda/n = g(\sin \theta_i + \sin \theta_d)$, where θ_i is the incidence angle, m is the diffraction order, and g is the groove spacing. If the refractive index n varies, then the angle of diffraction θ_d will vary and light of the same wavelength will not focus to the same spot. What matters is not the local variation of refractivity but rather its integral along the ray path.

If the refractive index is inhomogeneous then the wavefront arriving at the exit face of the grating will no longer be planar because different portions will arrive at different times. In principle one could record the wavefront error and use a computer controlled polishing technique like MRF (magnetorheological finishing) to compensate for the error by reshaping the exit face. Unfortunately the crystal stress varies with direction so the refractivity will depend the direction of the electric field with respect to the stress axes. So we can only correct for the wavefront error for a single polarization state. This puts a tight constraint on the maximum tolerable Δn . For a peak to valley wavefront error of $\lambda/4$ at the exit face, $\Delta n \leq \lambda/4d$. For a 30 cm path the maximum Δn across the crystal face will be 8.3×10^{-6} at $10 \mu\text{m}$ and 4.2×10^{-6} at $5 \mu\text{m}$. This can be relaxed slightly because most of the paths through the grating are much shorter than 30 cm. The preceding analysis shows that stress birefringence and refractive inhomogeneities can be severe problems for large immersion gratings. It is clearly required to reduce stress induced refractivity variations down to levels lower than are commonly achieved. There are several pathways forward.

It is known that the refractivity has a roughly parabolic profile¹². This follows the temperature distribution for a cylindrical body. If only the central 1/3 of a boule is used then the Δn is about 10% of that for the full diameter. Careful and slow annealing can reduce this still further. It is essential that an infrared interferometer/polarimeter be available to measure the residual birefringence and inhomogeneity. This will determine the efficacy of additional annealing cycles. The largest stress is in the radial direction. If the blank is cut so that the direction of propagation is along a boule radius, then the rays will only be affected by the much smaller tangential refractivity variations.

All the above applies for CZ grown material. It is possible that crystal grown by another technique known as float zone (FZ) may have lower stress. In the FZ process the raw material is heated by an induction coil which may produce a more uniform thermal distribution in the crystal than the radiatively heated CZ process. Measurements need to be made to test this hypothesis.

Unlike ordinary reflective gratings, immersion gratings are made of transmissive materials and must be coated. High reflectivity coatings are needed for the grating surface and an antireflection coating for the entrance and exit surfaces. Fortunately germanium is a commonly used infrared material and good antireflection coatings have been developed for the various windows of atmospheric transmission. The size of the prototype grating is not a concern given the size of coating chambers (> 30 inch diameter) currently used by vendors. Infrared instruments are generally operated at low temperatures to reduce thermal background photons so good adhesion is required down to cryogenic temperatures. Coating stress should be low to avoid any distortion in the shape of optical surfaces. Generally these issues are well understood.

Although good high reflectivity, dielectric coatings exist for germanium, a metallic coating is preferred for the grating surface. It is difficult to get good thickness control on inclined surfaces and infrared coatings are usually comprised of a number of thick (microns) layers. By comparison a metallic layer achieves high reflectivity in a single layer 100 to 200 nm thick. The tolerance is looser and there is less stress in a thin layer. More detail on metallic reflective coatings is given in Appendix A.

4. CURRENT MACHINING CAPABILITIES AT LLNL

Having explored materials issues concerning large germanium blanks, the next step in the feasibility study was to examine fabrication issues, the limits of machining both in terms of machine accuracy and workpiece size capability. Albert Michelson has said that cutting a diffraction grating is the most challenging task that one could demand from a mechanical device. The tolerances are measured in fractions of wavelengths of light and in the case of periodic or random errors in groove position, very small fractions of a wavelength. Grooves must be cut one at a time and sequentially leading to a prolonged machining operation. This puts extreme requirements on machine stability and isolation from environmental variations (e.g. diurnal temperature changes) and perturbations (e.g. extraneous vibrations). Nevertheless these requirements have been met for many years with one of a kind ruling engines. We have recently been successful in fabricating small area immersion gratings in germanium on one of LLNL's ultra-precision lathes. The challenge is to scale this process to much larger sizes.

4.1 Direct machining grating surface using LLNL's ultra-precision machine tools

Small germanium immersion gratings are an enabling technology for compact spectrometer designs that were created at LLNL several years ago. But a way had to be found to fabricate them to the required tolerances. Cornell had procured some test rulings in ZnS and ZnSe as precursors to possible grism development¹⁴. Our measurements on those rulings gave us optimism that commercial vendors could fabricate germanium gratings¹⁵.

LLNL engineers solicited an optics fabrication shop equipped with commercial diamond turning machines to produce proof-of-concept grating. Collaborative efforts worked to develop successful material removal parameters but could not arrive at cost effective solutions for meeting wavefront error and groove spacing requirements. Although the effort to use "as purchased" equipment failed, we later demonstrated that it is possible and practical to directly machine grating features across moderate areas (1cm x 1cm) to specification. LLNL's Precision Engineering Research Lathe (PERL II, figure 2) was retrofitted with hardware to perform the single crystal, diamond fly-cutting operation. The ultra-precision process uses a low speed (<1000 rpm) air-bearing spindle to spin the tool in a large arc. A 75 mm radius tool path removes a single ductile chip of germanium with each rotation. The spindle is supported by one of the machine's two hydrostatic linear slides. The machine's "X" axis supports and translates the grating substrate in a straight path under the rotating tool causing a groove to be cut. The spindle or "Z" axis is incremented by the grating pitch after cutting each groove. This machine has allowed us to manufacture thin (<25 mm) planar gratings. When tested with cutting cycles approaching 1 week in duration, the machine proved to have adequate stability and immunity to most environment influences.

Machine design criteria for manufacturing large area/long duty cycle optics rely on systems that include dynamic vibration isolation and closed loop, environmental temperature control. Acoustic and ground transmitted vibrations contribute to surface roughness and waviness. This disturbance and other sources of asynchronous motion are dampened by dynamic (air) machine isolators and liquid hydrostatic slide ways. Short scale (5 μm by 5 μm) surface roughness of approximately 1 nm (rms) can be achieved on the groove facets. Dimensional stability of critical machine structures provides global surface figure and groove spacing accuracy. Isolating the machine from internal and external thermal influences is accomplished through multiple temperature control systems. Liquid temperature control for isolating the machine from its own heat generating (air bearing) spindles and motors, and dual chamber, down draft, air shower systems for minimizing external influences including the radiant heat from the machine operator. All systems act to maintain absolute 20°C temperature to within $\pm 0.05^\circ\text{C}$. Interferometric control of both axes of translation establishes precise spacing from groove to groove.

LLNL has infrastructure in place for manufacturing small planar gratings. The PERL II machine has many design attributes that enhance its capability for manufacturing high quality gratings. Fabrication times can be long, limited by the small submicron chip thicknesses that can be removed while still maintaining the ductile regime and the modest 1000 rpm spindle speed. Retrofitting the machine with a high-speed cutting spindle can reduce cutting times. Commercially available units can increase the current cutting speed by two orders of magnitude (>100k RPM).

4.2 LLNL's capabilities for producing large ultra-precision gratings

Despite its excellent performance at fabricating small gratings, the PERL-II simply does not have the capacity to handle a large grating like the one under study. Its translation stages have a maximum travel of 10 cm. Furthermore there is only a 10 cm clearance between the spindle axis and the workpiece translation stage. This is insufficient space to fit a large grating blank and allow an adequate swing radius for the diamond tool. Commercial diamond turning machines are available with at least 40 cm travel and a 40 cm diameter workspace. However they lack interferometric position control and built in environmental isolation and were not considered further.

LLNL's Large Optics Diamond Turning Machine (LODTM) was constructed in the early 1980's to fabricate large aspheric mirrors for DARPA. It is a vertical axis machine (see figure 3) with a 160 cm diameter x 51 cm work volume, and could potentially fabricate large area gratings. LODTM has technology similar to PERL but takes advantage of low (thermal) expansion materials and an independent Super Invar metrology frame. LODTM's accuracy is enhanced by having seven laser interferometer systems for guidance and positioning. The interferometers operate in vacuum, immune from environmentally induced variations in atmospheric refractive index. The minimum programmable increment of tool motion is 3 nm, the same as PERL. LODTM is capable of producing optical surfaces with an rms surface figure error of 28 nm over the full working volume.

Because of its much larger size the LODTM spindle rotates at a much lower speed than PERL, 50 rpm vs. 1000 rpm. So it was clear that the machining configuration used to cut gratings on PERL would not be applicable to LODTM. Instead we chose to make use of some of the unique features of LODTM. Figure 4, a cutaway drawing of the machine, shows a horizontal working surface rotating around the vertical "C" axis. The tool bar, supported by the upper structure and extending vertically downward toward the working surface, can be precisely moved under interferometric control in the X, Y or Z directions. Here we define Z as the vertical direction, parallel to the spindle or C axis, and X and Y are in the horizontal plane.

The work plan and layout (figure 5) show the grating substrate supported by the "tool bar". This configuration locates the substrate's grating "plane" in a position that best takes advantage of the machine's laser positioning system. This minimizes the effects of machine errors, maximizing pitch spacing precision, and profile accuracy. The cutting tool is fitted to a precision, high-speed spindle, which is supported by the machine's main vertical axis spindle. The high-speed spindle is rotated back and forth about a large radius (R) while its angular position about the C-axis is tracked. The tool bar (substrate) is shifted using the "X" axis as the substrate passes by the fly-cutter. This "X-C" CNC compensated program is used to produce straight grating features in the substrate. To cut successive grooves, the tool bar must be incremented in X to obtain the required grating pitch as well as in Z so that the tool clears the previous groove. See figure 6.

We produced a documented working plan for fabricating large, immersion gratings on LODTM. Within the work plan there are costs and timelines for procuring systems, manufacturing hardware, producing test articles and qualifying the results. Limitations for making large gratings on LODTM include; the mass of the grating as the machine's servo system and "Z" axis tool bar counter balance is designed for a specific mass.¹

4.3 Metrology

A common saying in the ultra-precision machining world is that "you can't make what you can't measure." In other words ultra-precision machining is of little use without ultra-precision metrology to determine that the specifications have been met. Testing a diffraction grating as a grating (i.e. using it in a spectrometer) is the most comprehensive test, but often requires a lot of expensive ancillary hardware (e.g. spectrometer optics, focal plane array with readout electronics, cryogenics, etc.). We have several other methods for assessing grating performance. An interferometric test of the diffracted wavefront provides one of the best tests of performance. A 633 nm HeNe laser and a rotation stage can be used to determine blaze angle and groove spacing. It also gives some indication of the level of scatter. Atomic force microscopy (AFM) and micro phase measuring interferometers are used to quantify the individual grating facets for smoothness/flatness, internal corner radius and external edge sharpness. Optical microscopy has a role in detection of gross defects. All of these techniques with the possible exception of AFM are usable with large gratings.

5. FUTURE MACHINING CAPABILITIES AT LLNL

As machining requirements shift from pure research and one of a kind fabrications to low volume production (e.g. laser fusion targets), LLNL is gradually replacing its older custom-made diamond turning machines with newer commercial machines that offer a more economical path toward precision manufacturing. However in some cases the result is a loss of capability in size and weight capacity and/or accuracy. It was decided several years ago to develop a new machine, the Precision Optical Grinder and Lathe (POGAL), which simultaneously provides better accuracy and finish than individually possible with our current or commercial diamond turning machines (see figure 7 for a solid model of the POGAL). In addition, it offers greater flexibility provided by B and C rotary axes (i.e. the cutting tool can move in a circular path as well as a linear one) and the capability to grind as well as diamond turn. We aggressively set target specifications at 10 nm rms accuracy over 400 mm diameter by 400 mm long part and surface finish less than 1 nm rms. It incorporates many of the same techniques used on LODTM to achieve 25 nm rms accuracy over a much larger work space.

In the years since development started the machine base and slides have been constructed (see figure 8) and key aspects of the controller have been demonstrated. The overall architecture of the machine has been determined but

¹ LODTM was originally designed to carry a fast tool servo weighing approximately 10 lbs.

considerable detailed engineering remains to be done. Completion will likely occur in two major steps: 1) achieving functional parity with the commercial machines and 2) enhancing accuracy by upgrading with a metrology frame and implementation of full tool-point correction (i.e. closed loop, real time, active control of tool position). The timeline for completion depends on available funding but is expected to take several more years. When the POGAL is fully operational it will be the optimal machine to fabricate large immersion gratings similar to those discussed in this paper.

6. CONCLUSIONS

We have carried out a design study of the issues involved in the fabrication of a large germanium immersion grating. Although previous successful fabrications of smaller gratings have used the PERL-II ultra-precision lathe, it does not have the size capacity to handle a large grating blank. The LODTM has much larger capacity and superb stability and could certainly handle the job, although some modifications would be required (i.e. adding an auxiliary spindle). For the longer term the tighter specifications POGAL machine, currently under development, would make it a better choice. There is some concern about the stress-induced birefringence and refractive index inhomogeneities present in large germanium crystals. The capability to measure these parameters is essential. The blank will need to be carefully selected and additional annealing may well be required.

7. ACKNOWLEDGEMENTS

Thanks to are due to Michael Chrisp for illuminating discussions on the effects of birefringence and refractive inhomogeneity on optical performance. This work was performed under the auspices of the U.S. Department of Energy by University of California, Lawrence Livermore National Laboratory under Contract W-7405-Eng-48.

8. REFERENCES

1. E. Hulthen and H. Neuhaus, "Diffraction Gratings in Immersion," *Nature* **173**, pp. 442-443, 1954
2. P. J. Kuzmenko, P. J. Davis, S. L. Little, L. M. Little and J. V. Bixler, "High efficiency germanium immersion gratings," paper 6273-147, this conference.
3. N. Ebizuka, S. Morita, T. Shimizu, Y. Yamagata, H. Omori, M. Wakaki, H. Kobayashi, H. Tokoro and Y. Hirahara, "Development of immersion grating for mid-infrared high dispersion spectrograph for the 8.2m Subaru telescope," in *Specialized Optical Developments in Astronomy*, E. Atad-Ettinger and S. D'Odorico editors. Proceedings of SPIE Vol. 4842, pp.293-300, 2003.
4. Yasui, C., Ikeda, Y., Kondo, S., Motohara, K., and Kobayashi, N., "Instrument Design of Warm INfrared Echelle Spectrograph (WINERED)", in *Instrumentation for Extremely Large Telescope*, Eds. Tom Herbst, Wolfgang Gaessler, 2006
5. D. McDavitt, J. Ge, S. Miller and J. Wang, "Silicon immersion gratings for very high resolution infrared spectroscopy," in *Optical Fabrication, Metrology, and Material Advancements for Telescopes*, E. Atad-Ettinger and P. Dierickx editors. Proceedings of SPIE Vol. 5494, pp.536-544, 2004.
6. E. D. Palik, *Handbook of Optical Constants of Solids*, Academic, Orlando, 1985.
7. S. J. Fray, F. A. Johnson, J. E. Quarrington and N. Williams, "Lattice bands in germanium," *Proceedings of the Physical Society of London* **85**, pp. 153-158, 1965.
8. T. F. Deutsch, "Laser window materials - an overview," *Journal of Electronic Materials* **4**, pp.663-725, 1975.
9. J. L. Pankove, *Optical Processes in Semiconductors*, Prentice Hall, Englewood Cliffs, New Jersey, 1971.
10. R. E. Gaskin and C. Lewis, "Interferometric measurement of refractive index variations in infra-red transmitting materials at 10.6 μm ," *Optica Acta* **27**, pp. 1287-1294, 1980.
11. G. Gafni, M. Azoulay, C. Shiloh, Y. Noter, A. Saya, H. Galron and M. Roth, "Large diameter germanium single crystals for infrared optics," *Optical Engineering* **28**, pp.1003-1008, 1989.
12. B. Depuydt, P. Boone, P. Union, P. Muys, D. Vyncke and Claus Goessens, "Interferometrical characterization of stress birefringence in germanium," *Proceedings of SPIE Vol. 3098*, pp.559-565, 1997
13. C. Poznik, Umicore Corp. private communication, 2005.
14. J.D. Smith, S.A. Rinehart, J.R.Houck, J.E. Van Cleve, J.C. Wilson, M. Colonno, J. Schoenwald, B. Pirger and C. Blacken, "SCORE 1+: Enhancing a Unique Mid-Infrared Spectrograph," in *Infrared Astronomical Instrumentation*, Albert M. Fowler, Editor, *Proceedings of SPIE Vol. 3354*, pp.798-809 (1998).

15. P. J. Kuzmenko, L. M. Little, P. J. Davis and S. L. Little, "Modeling, Fabrication and Testing of a Diamond-Machined Germanium Immersion Grating," in *IR Space Telescopes and Instruments*, Proceedings of SPIE Vol. 4850, pp.1179-90 (2002).
16. G. M. Smith, D. V. Forbes, R. M. Lammert and J. J. Coleman, "Metallization to asymmetric cladding separate confinement heterostructure lasers," *Applied Physics Letters*, vol. 67, No. 26, pp.3847--9 (1995).
17. J. Hoffman and W. Wolfe, "Cryogenic refractive indices of ZnSe, Ge and Si at 10.6 microns," *Applied Optics* vol. 30, pp.4014 (1991).

APPENDIX 1. REFLECTIVE COATINGS FOR IMMERSION GRATINGS

Metal coatings offer several advantages. The technology of evaporating or sputtering metals is simple and mature. Only relatively thin coatings (< 150 nm) are required to achieve full reflectivity so the effects of coating stress are usually negligible. Metallic coatings are broadband, show little polarization sensitivity, and have high reflectivity. However, when used in immersion a metal will have a lower reflectivity than when used in air.

Infrared spectrometers are often operated at cryogenic temperatures to reduce the level of background radiation. Since germanium has a thermal expansion coefficient much lower than that of most metals there can be a thermal mismatch and a tendency for the coating to peel off under thermal cycling. This is of special concern with noble metals like gold that tend to have poor adhesion. Typically a thin intermediate layer like chromium, nickel or titanium are used to enhance adhesion. The adhesion layers tend to have lower electrical conductivity and hence higher optical loss than the reflective layers. So it is important to keep the adhesion layer as thin as possible. Work with GaAs waveguide lasers show that as little as 1 nm of titanium is an adequate adhesion layer for gold and that reflective losses increase with increasing titanium thickness¹⁶. We typically use 5 nm of chromium under 100 to 200 nm of gold. A germanium wafer to which a chrome/gold coating has been sputtered can be repeatably plunged into liquid nitrogen without damage or peeling.

Table 2 below lists reflectivities in air and immersed in germanium for several common metals near 10 μm . We calculated normal incidence reflectivities using tabulated values of optical constants⁶ and values of the refractive index of germanium at 50 K and at 300 K measured by Hoffman and Wolfe¹⁷. Aluminum gives the immersed reflectivity among common metals. Lithium gives the highest immersed reflectivity of all. However, there may be issues with deposition and adhesion. It is a reactive material and would definitely need a protective coating.

Table 2 Immersed Reflectivity for several metals

		Al		Ag		Au		Li	
		n	k	n	k	n	k	n	k
	n@10.6 μm	26.6	92.2	13.11	53.71	12.24	54.71	0.659	38
air	1	0.989		0.983		0.985		0.998	
Ge (50 K)	3.93	0.956		0.935		0.941		0.993	
Ge (300 K)	4.03	0.955		0.934		0.939		0.993	

Figure 9 plots the calculated immersed reflectivity of a Cr/Au coating on germanium as a function of the chromium thickness. A 5 nm adhesion layer of Cr decreases reflectivity by about 1% compared to gold alone.

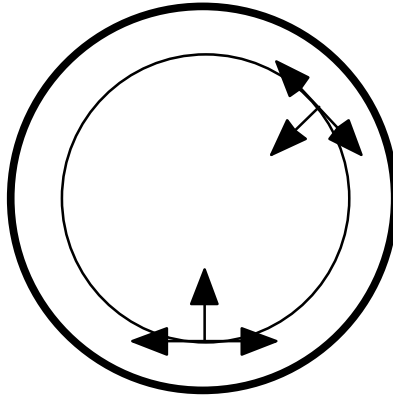


Figure 1. This diagram shows the stress in single crystal germanium. The view is in a plane normal to the crystal pull direction. The arrows indicate the local stress axes. There is compressive radial stress and tensile tangential stress.

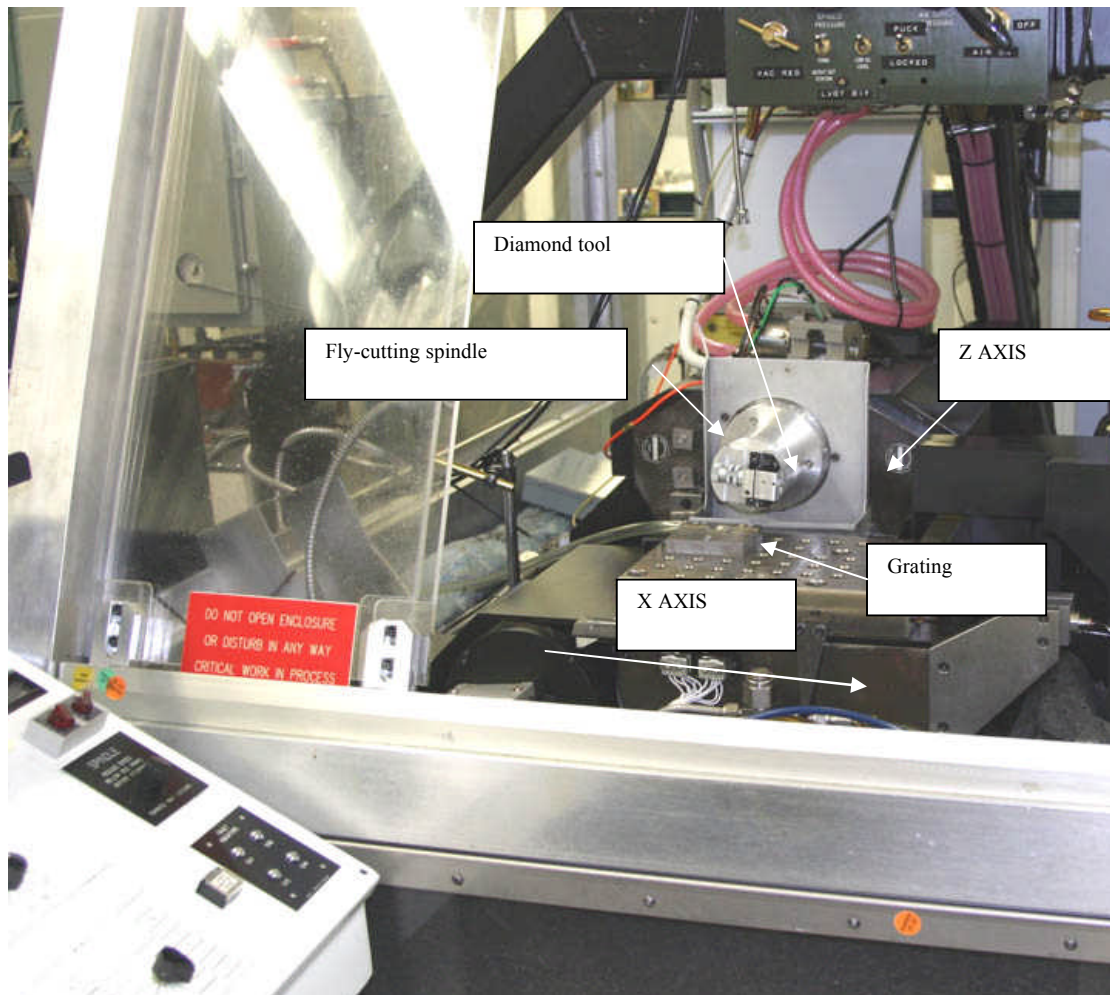


Figure 2. Here is the PERL-II setup for flycutting a grating. The small germanium substrate is waxed down to a steel block, which is fastened to the X translation stage. It slides slowly under the rotating tool to cut a groove.



Figure 3. This is the Large Optics Diamond Turning Machine (LODTM) in its environmentally controlled room. The large work volume at the center is clearly visible.

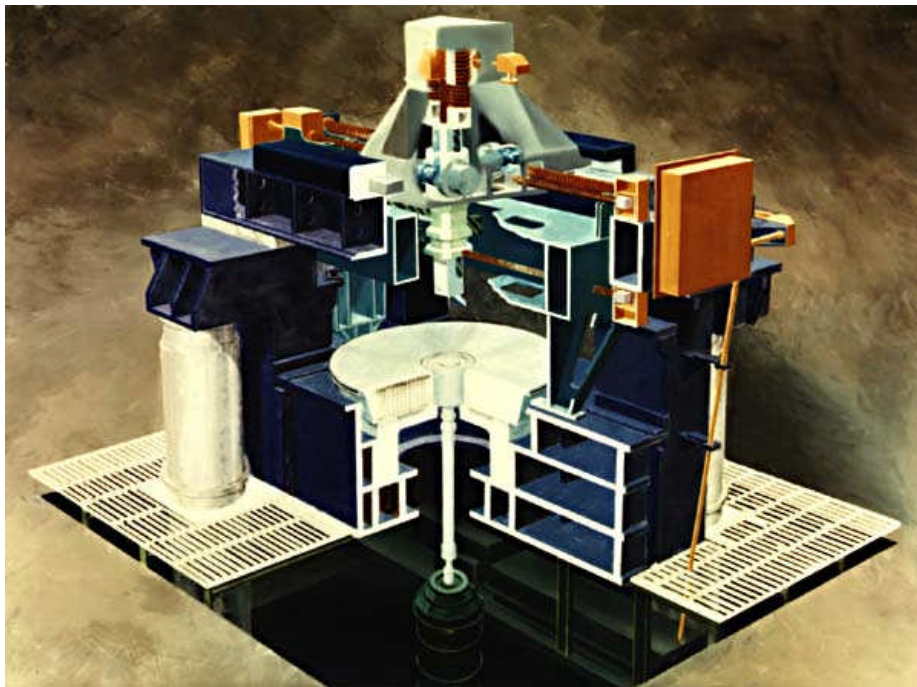


Figure 4. This cutaway drawing of LODTM shows some of its features including its main vertical axis and the toolbar supported by the overhead structure.

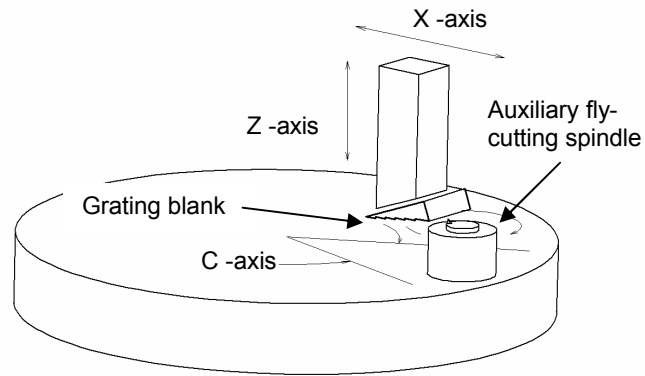


Figure 5. This is the LODTM setup for cutting a large grating. An auxiliary flycutting spindle that holds the diamond tool bit is mounted to the large spindle face that rotates about the C axis.

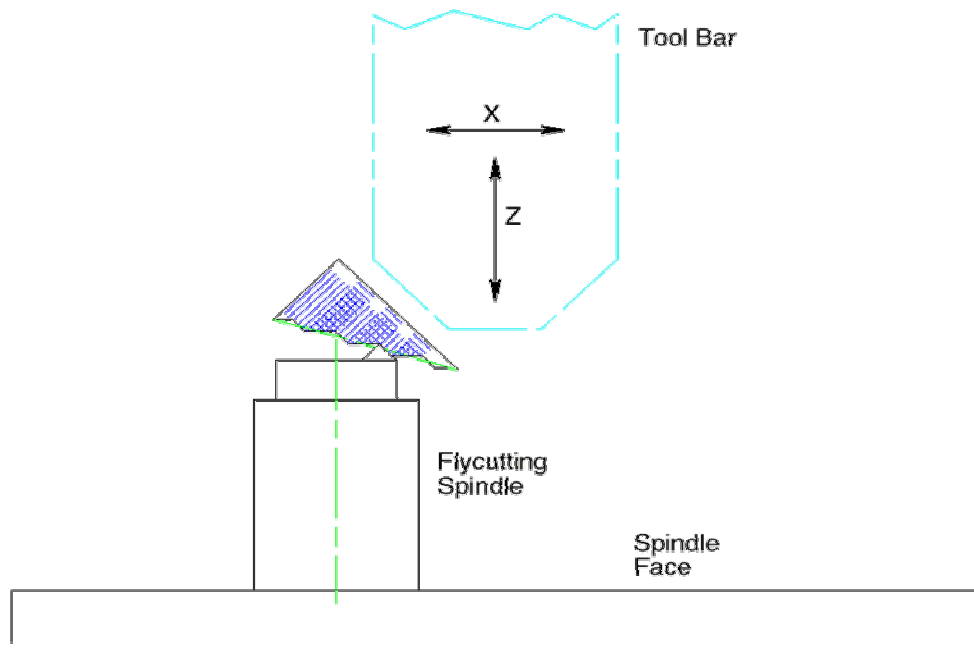


Figure 6. Here is more detail of the cutting process. The flycutting spindle moves along a circular path as the large spindle rotates back and forth. Fast compensation by toolbar motion in the x-direction keeps the grooves straight. To cut successive grooves the toolbar is stepwise incremented both in X and Z.

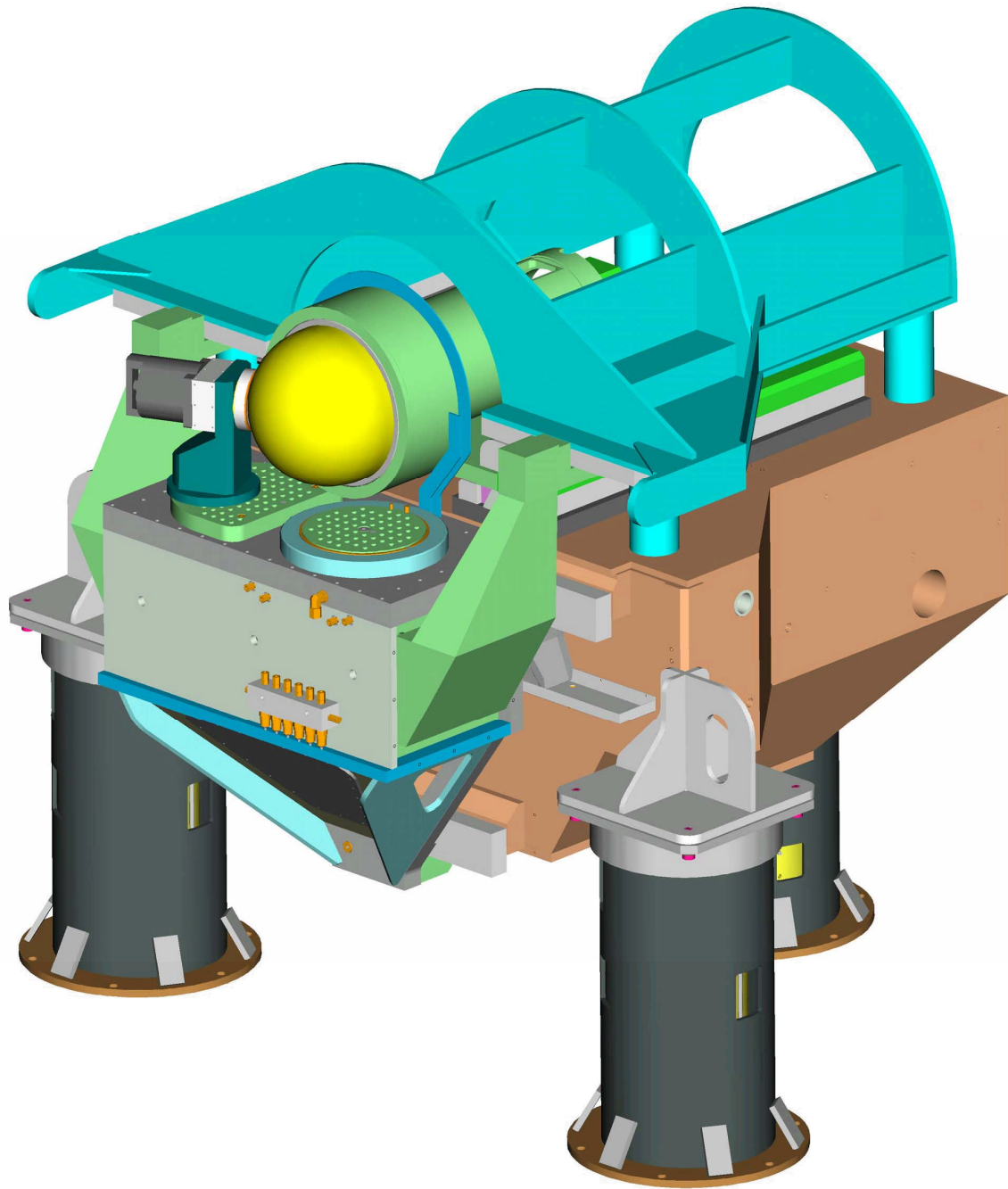


Figure 7. Solid model of POGAL showing a notional design of the metrology frame above the machine base. The width of the base is about 60" and the length of the base is about 50". The width of the slide hanging from the front is 32" and it overhangs about 18". The range of travel is 16" in the z-direction, along the spindle axis and 14" in the x-direction, transverse to the spindle axis.



Figure 8. POGAL base and slides during construction at Moore Special Tool Company.

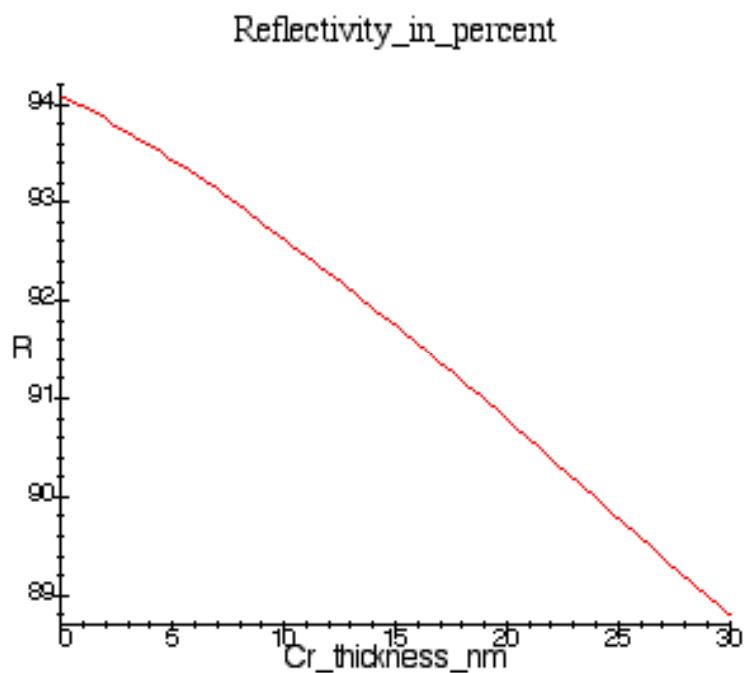


Figure 9. Plot of calculated normal incidence immersed reflectivity of gold on germanium with a thin adhesion layer of chromium. The reflectivity is plotted vs. thickness of the chromium layer.